Proceedings of the 2001 IEEE
International Conference on Robotics & Automation
Seoul, Korea • May 21-26, 2001

Analysis on Detaching Assist Motion (DAM)

Makoto Kaneko, Tatsuya Shirai, Kensuke Harada, and Toshio Tsuji

Faculty of Engineering
Hiroshima University
1-4-1 Kagamiyama, Higashi-Hiroshima, Hiroshima 739-8527, JAPAN

Abstract

Through grasp experiments by human, we found an interesting grasping pattern, where human easily captures a small object placed on a table within the hand by changing the finger posture from upright to curved ones after each finger makes contact with the object. A series of this motion is called as Detaching Assist Motion (DAM). This paper discusses a condition for achieving DAM by taking the idea of Self-Posture Changing Motion (SPCM). A sufficient condition for lifting up the object from the table is discussed. Some experiments are also shown to verify the condition.

1 Introduction

Multi-fingered robot hands have a potential advantage to perform various skillful tasks like human hands. For considering the grasp strategy of robot hand, human motion often provides us with good hints[1]–[5]. Cutkosky[1] has analyzed manufacturing grips and correlation with the design of robot hands by examining grasps used by humans working with tools and metal parts. Bekey et al.[2] have presented the automatic grasp planner which generates an order set of grasp according to task description, heuristics, and geometry of an object. Kang and Ikeuchi[3] have proposed the *contact web* and the *grasp cohesive index* for automatic classification of human grasping. Saito and Nagata[5] have proposed a method to classify and describe grasping and manipulation. While these works[1]–[5] discussed the classification of either final grasp patterns or grasp postures, we are particularly interested in considering the whole grasping procedure where the hand approaches an object placed on a table and finally achieves an enveloping grasp. Through the observation of human grasping, we found that human changes his (her) grasping strategy according to the size of objects, even though they have similar geometry. We called the grasp planning *Scale-Dependent Grasp*[6]–[11]. Through these works, we found that human roughly switches the grasp pattern three times, as the size increases. The most complicated pattern is observed for an object whose representative size is smaller than that of our finger tip, while a simple grasp pattern can work for a relatively large object.

In this work, we focus on cylindrical objects whose diameter is relatively small as shown in Fig.1. For such objects, two characteristic patterns are observed. One is that human first picks up the object from the table, and then finally achieves the target grasp through a grasp transition from the fingertip to the enveloping grasps, as shown in Fig.1(a). Most of us take this pattern. The other one which is observed just by chance is that human first approaches the object until finger tips make contact with the object, and then the finger posture is changed from upright to curved ones gradually, as shown in Fig.1(b). This is what we call *Detaching Assist Motion (DAM)*. From the viewpoint of robot application, the most attractive feature of *DAM* is its extremely simple finger motion, while the grasp pattern in Fig.1(a) is so complicated that the robot hand may often fail especially in changing the phase from fingertip to envelope grasps. The second advantage is that the *DAM* is achieved on the table in most phases and, therefore, it is not necessary to worry about dropping the object. Our goal is to analyze the *DAM*, especially to explore under what condition a robot hand can lift up an object from the table. During the *DAM*, either sliding or rolling motion may happen at the contact point. We do not care what kinds of motion occur but are interesting only to know whether the object is lifted up or not.

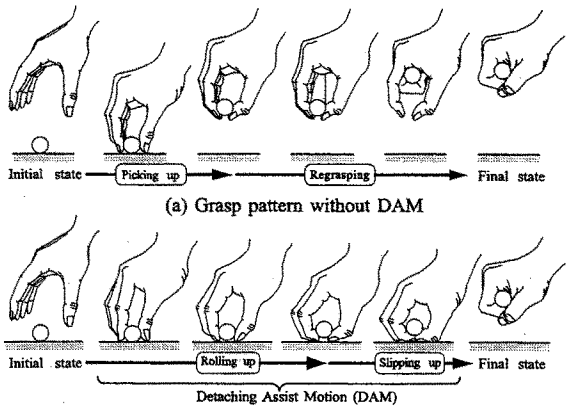

(a) Grasp pattern without DAM

(b) Grasp pattern with DAM

Fig. 1: Two grasp strategies for enveloping a cylindrical object placed on a table

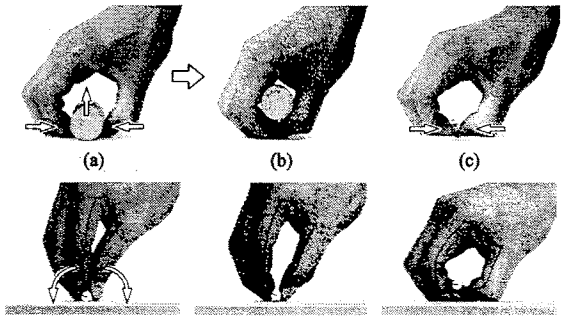

(d) DAM for a small object

Fig. 2: Grasping motion by human

This paper is organized as follows. In section 2, we explain the basic working mechanism of *DAM*. In section 3, we show that the *DAM* can be explained by the *Self–Posture Changing Motion (SPCM)*, and explore a sufficient condition for always lifting up the object from a table by utilizing the *SPCM*. In section 4, we implement the *SPCM* into the grasping procedure of a three-fingered robot hand, and confirm that the *DAM* effectively works for cylindrical objects with various size, shape and contact friction. Finally, in section 5, we conclude our work.

2 Detaching Assist Motion (DAM)

2.1 What is DAM?

An enveloping grasp can be achieved by the following three fundamental phases: detaching an object from a table, lifting it up toward the palm, and firmly grasping. For detaching the object whose size is larger than fingertip, a human often utilizes the *wedge–effect* where a simple pushing motion of the bottom part of object makes the object detach from the table as shown in Fig.2(a) and (b)[6]. Due to its simple motion planning, we can easily implement it into the grasping procedure of a multi–fingered robot hand. Either under significant friction or for an object with small diameter, we can not detach the object by using the *wedge–effect*, since the finger forces balance within the object and do not produce a lifting force any more as shown in Fig.2(c). Even under such a situation, human can easily envelop the object. Most of us first pick up the object from the table and achieve the target grasp through regrasping process from the fingertip to the enveloping grasps. Just by chance, we found an interesting grasp pattern where human can capture the object by simply changing finger posture from upright to crooked ones as shown in Fig.2(d). The series of motion is called as *Detaching Assist Motion (DAM)*. We would note that either a rolling or a sliding motion or perhaps both occur at the point of contact between the object and the fingertips.

2.2 Basic Working Mechanism of DAM

Let us consider what happen during the *DAM* by using the fingertip model as shown in Fig.3. We assume

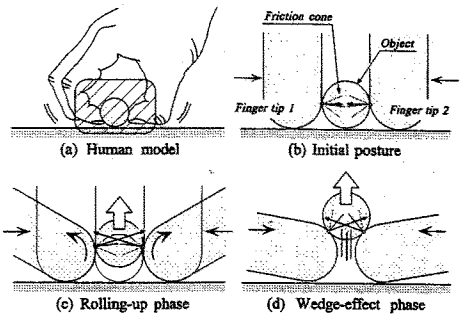

Fig. 3: The basic mechanism of DAM

that the object is small enough to ensure that a simple pushing motion in the horizontal direction can not lift up the object as shown in Fig.3(a). Further, we simplify the fingertip model as shown in Fig.3(b). If each fingertip does not slip on the surface of object, the object will be lifted up according to the geometrical constraint between the fingers and the object as shown in Fig.3(b) and (c), while both fingertips rotate from the initial to the final postures. We call this phase *Rolling–up phase*. As the object is lifted up, the normal direction of friction cone gradually changes upwards while the contact point moves towards the bottom of object. Finally, the moment the contact force is away from the friction cone, the object slips on the surface of fingertips. Once the contact force is away from the boundary, the *wedge–effect* effectively helps to move up the object as shown in Fig.3(d). We call the final phase *Wedge–effect phase*. These are the outline of the working mechanism of *DAM*. The phase from *Rolling–up* to *Wedge–effect* is automatically switched depending upon the contact friction as well as the finger rotating motion.

3 How can a Robot Achieve DAM ?

3.1 SPCM can Simulate DAM

While several strategies for robot hands which are equivalent to the human *DAM* can be considered, we utilize compliant motion of link system having one compliant joint (*s-th*) and one position–controlled joint (*p-th*) as shown in Fig.4(a). Now, suppose that we impart an arbitrary angular displacement $\Delta\theta_p$ at the position–controlled joint for such a link system contacting with an environment. Under the condition, the link system will automatically change its posture while keeping contact between the environment and the link system, if $\Delta\theta_p$ is given appropriately. This series of motion is termed as *Self–Posture Changing Motion (SPCM)*[12], [13]. *SPCM* has been conveniently utilized for detecting an approximate contact point between a link system and an unknown object under the assumption that the object does not move during sensing. For example, let us consider two different link postures during *SPCM*. Between two link postures, we can always find an intersection, which provides us with an approximate contact point. This approach allows

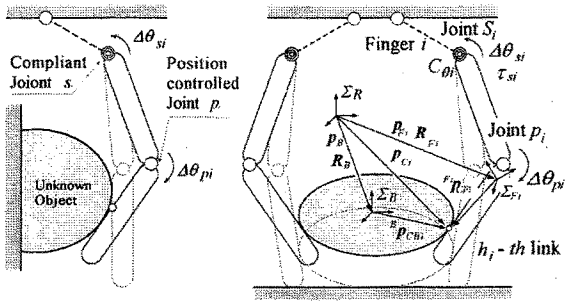

(a) Object is fixed (b) Object's motion is allowed

Fig. 4: Self-Posture Changing Motion

us to detect an approximate contact point without implementing any tactile sensor, which is a great advantage. In this work, however, we allow the object to move according to the contact force imparted by the link as shown in Fig.4(b).

Nomenclature

Σ_R	Coordinate system fixed at the base.
Σ_B (Σ_{Fi})	Coordinate system fixed at the center of gravity of object (at i-th finger link).
$\boldsymbol{p}_B$ ($\boldsymbol{p}_{Fi}$)	Position vector of Σ_B (Σ_{Fi}) with respect to Σ_R.
$\boldsymbol{R}_B$ ($\boldsymbol{R}_{Fi}$)	Rotation matrix of Σ_B (Σ_{Fi}) with respect to Σ_R.
$\boldsymbol{p}_{Ci}$	Position vector of i-th contact point with respect to Σ_R.
${}^B\boldsymbol{p}_{CBi}$ (${}^{Fi}\boldsymbol{p}_{CFi}$)	Position vector of i-th contact point with respect to Σ_B (Σ_{Fi}).
$C_{\theta i}$	Compliance of s_i-th joint of i-th finger.
$\boldsymbol{K}_\theta$	Stiffness matrix of compliant controlled joints. $\boldsymbol{K}_\theta = diag[k_{\theta 1}, \ldots, k_{\theta n}]^t \in R^{n\times n}$ where $k_{\theta i} = 1/C_{\theta i}$.
$\Delta\theta_{pi}$	Angular displacement for p_i-th joint of i-th finger ($i = 1, \ldots, n$).
$\Delta\boldsymbol{\theta}_p$	Angular displacement vector of position–controlled joints. $\Delta\boldsymbol{\theta}_p = [\Delta\theta_{p1}, \ldots, \Delta\theta_{pn}]^t \in R^{n\times 1}$.
$\Delta\theta_{si}$	Angular displacement for s_i-th joint of i-th finger ($i = 1, \ldots, n$).
$\Delta\boldsymbol{\theta}_s$	Angular displacement vector of compliant–controlled joints. $\Delta\boldsymbol{\theta}_s = [\Delta\theta_{s1}, \ldots, \Delta\theta_{sn}]^t \in R^{n\times 1}$.
n_{CBi} (n_{CFi})	Unit normal vector directing outside at i-th contact point on the surface of object (i-th finger).
$S_B({}^B\boldsymbol{p})$ ($S_{Fi}({}^{Fi}\boldsymbol{p})$)	Function representing the surface shape of object (i-th finger link).
$\boldsymbol{f}_c$	Contact force vector at each contact point. $\boldsymbol{f}_c = [\boldsymbol{f}_{c1}^t, \ldots, \boldsymbol{f}_{cn}^t]^t \in R^{3n\times 1}$.
$\boldsymbol{W}_{ext}$	Load wrench. $\boldsymbol{W}_{ext} \in R^{6\times 1}$.

[Definition of *SPCM*]

For a link system with m joints, suppose that the s-th joint is compliant and $h(> s)$-th link makes contact with an object, and the angular displacement,

$$|\Delta\theta_p| \neq 0 \tag{1}$$

is imparted at the position–controlled joint p ($h \geq p > s$). If the vector $\boldsymbol{p}_C \in R^{3\times 1}$ satisfying the following equations is always found during a change of link posture, we call there exists *Self–Posture Changeability (SPC)*.

$$S_B({}^B\boldsymbol{p}_{CB}) = 0, S_F({}^F\boldsymbol{p}_{CF}) = 0 \tag{2}$$

$$\boldsymbol{p}_B + \boldsymbol{R}_B{}^B\boldsymbol{p}_{CB} = \boldsymbol{p}_F + \boldsymbol{R}_F{}^F\boldsymbol{p}_{CF} = \boldsymbol{p}_C \tag{3}$$

$$\boldsymbol{n}_{CB} = -\boldsymbol{n}_{CF} \tag{4}$$

The series of motions that bring about a *SPC* is defined as a *Self–Posture Changing Motion (SPCM)* and we express it as $SPCM\{k_\theta, \Delta\theta_p\}$, where k_θ is the joint stiffness of the s-th joint.

In *SPCM*, the h-th link always keeps contact with the object during the change of link posture. From the basic behavior, we can see that it is almost equivalent to the *DAM* by human. The *SPCM* has an advantage where it can achieve with, at least, one compliant joint and one position–controlled joint at each finger without complicated motion planning.

3.2 A Sufficient Condition for Lifting Up an Object

Now, we discuss a sufficient condition for lifting up an object by utilizing the *SPCM*. Suppose that the robot hand utilizes $SPCM\{\boldsymbol{K}_\theta, \Delta\boldsymbol{\theta}_p\}$ for the object whose mass is m_B, where we use $\boldsymbol{K}_\theta$ and $\Delta\boldsymbol{\theta}_p$ for multiple fingers instead of k_θ and $\Delta\theta_p$. The equation of the force and the moment balancing on the object can be expressed as

$$\boldsymbol{W}_{ext} = -\boldsymbol{G}^t\boldsymbol{f}_c, \tag{5}$$

where $\boldsymbol{G}^t \in R^{6\times 3n}$ is the grasp matrix and given by

$$\boldsymbol{G}^t = \begin{bmatrix} \boldsymbol{I}_3 & \cdots & \boldsymbol{I}_3 \\ (\boldsymbol{R}_B{}^B\boldsymbol{P}_{CB1}\times) & \cdots & (\boldsymbol{R}_B{}^B\boldsymbol{P}_{CBn}\times) \end{bmatrix}$$

Suppose that the load wrench is $\boldsymbol{W}_{ext} = [0, 0, -(m_B g + f_{ez}), 0, 0, 0]^t$, where g and f_{ez} are the acceleration of gravity and the virtual force in the gravitational direction at the center of gravity of object, respectively. Any component of $\boldsymbol{f}_c$ can not exist outside of the friction cone at each contact point. If all components of $\boldsymbol{f}_c$ exist inside of the friction cone with $f_{ez} = 0$, the object does not move since the resultant force acting on the object balances within the object.

If the resultant force does not balance without pushing down by an additional force $f_{ez} > 0$, the object is necessarily lifted up from the table when such a virtual external force f_{ez} is removed. Based on this consideration, we can summarize the problem as follows.

[Problem formulation]

> For all possible contact forces within friction cone, search $SPCM\{\boldsymbol{K}_\theta, \Delta\boldsymbol{\theta}_p\}$ satisfying $c_z^t \Sigma \boldsymbol{f}_{ci} - m_B g > 0$ where c_z is the unit vector indicating the direction of z-axis in Σ_R.

Let $\boldsymbol{\tau}_s = [\tau_{s1}, \ldots \tau_{sn}]^t \in R^{n\times 1}$ be the torque at compliant joints. All compliant joints rotate $\Delta\boldsymbol{\theta}_s$ according to the angular displacement $\Delta\boldsymbol{\theta}_p$ under the assumption that the object does not move for an $SPCM\{\boldsymbol{K}_\theta, \Delta\boldsymbol{\theta}_p\}$. Under the $SPCM\{\boldsymbol{K}_\theta, \Delta\boldsymbol{\theta}_p\}$, $\boldsymbol{\tau}_s = -\boldsymbol{K}_\theta \Delta\boldsymbol{\theta}_s (= \boldsymbol{\tau}_{bias})$, where $\boldsymbol{\tau}_s = \mathbf{o}$ is assumed in the initial state. The relationship between τ_{si} and $\boldsymbol{f}_{ci}$ is given by $\tau_{si} = \boldsymbol{J}_i^t \boldsymbol{f}_{ci}$ where $\boldsymbol{J}_i^t \in R^{1\times 3}$ denotes the Jacobian matrix mapping from $\boldsymbol{f}_{ci}$ to τ_{si}. The contact force $\boldsymbol{f}_{ci}$ can be solved

$$\boldsymbol{f}_{ci} = [\boldsymbol{J}_i^t]^{\#} \tau_{si} + [\boldsymbol{I}_3 - (\boldsymbol{J}_i^t)^{\#} \boldsymbol{J}_i^t] \boldsymbol{w}_i \tag{6}$$

where $\boldsymbol{w}_i \in R^{3\times 1}$, $\boldsymbol{I}_3 \in R^{3\times 3}$ and $\#$ are an arbitrary vector, the identical matrix and the seudo–inverse matrix, respectively. τ_{si} is automatically determined when both $\boldsymbol{K}_\theta$ and $\Delta\boldsymbol{\theta}_p$ are given. The first term in eq.(6) denotes the force component perpendicular to both the unit axis vector of compliant joint and the vector indicating from the compliant joint to the contact point. The second term in eq.(6) is perpendicular to $(\boldsymbol{J}_i^t)^{\#}\tau_s$ and can take an arbitrary value within the friction cone. Now, we consider the frictional constraint. In order to change from nonlinear to liner constraint, a friction cone is often modeled by the L–faced polyhedral convex cone[8][9] whose span vectors are expressed by $\boldsymbol{v}^1, \ldots,$ and $\boldsymbol{v}^L$, respectively. The contact force for the i-th finger is given by

$$\boldsymbol{f}_{ci} = \boldsymbol{V}_i \boldsymbol{\lambda}_i \tag{7}$$

where $\boldsymbol{\lambda}_i = [\lambda_i^1, \ldots, \lambda_i^L]^t \in R^{L\times 1}$ and $\boldsymbol{V}_i = [\boldsymbol{v}_i^1, \ldots, \boldsymbol{v}_i^L] \in R^{3\times L}$. Therefore, the torque of compliant joint is expressed by

$$\tau_{si} = \boldsymbol{J}_i^t \boldsymbol{V}_i \boldsymbol{\lambda}_i \tag{8}$$

For n fingers, we obtain

$$\boldsymbol{\tau}_s = \boldsymbol{J}^t \boldsymbol{V} \boldsymbol{\lambda} \tag{9}$$

By solving eq.(9) with respect to $\boldsymbol{\lambda} = [\boldsymbol{\lambda}_i^t, \ldots, \boldsymbol{\lambda}_n^t]^t \in R^{Ln\times 1}$,

$$\boldsymbol{\lambda} = \boldsymbol{H}^{\#} \boldsymbol{\tau}_s + (\boldsymbol{I}_{Ln} - \boldsymbol{H}^{\#} \boldsymbol{H}) \boldsymbol{x} \tag{10}$$

where

$$\boldsymbol{H} = \begin{bmatrix} \boldsymbol{J}_1^t \boldsymbol{V}_1 & & \mathbf{o} \\ & \ddots & \\ \mathbf{o} & & \boldsymbol{J}_n^t \boldsymbol{V}_n \end{bmatrix}, \tag{11}$$

$\boldsymbol{x} \in R^{Ln\times 1}$ denotes an arbitrary vector. Eq.(10) can be rewritten as follows,

$$\boldsymbol{\lambda} = \boldsymbol{H}^{\#} \boldsymbol{\tau}_s + \boldsymbol{N} \boldsymbol{\Phi} \tag{12}$$

where $\boldsymbol{\Phi} \in R^{(L-1)n\times 1}$ is an arbitrary vector and $\boldsymbol{N} \in R^{Ln\times(L-1)n}$ is the full rank matrix satisfying $\boldsymbol{HN} = \mathbf{o}$. As a result, the total force of the center of gravity of object is expressed by

$$\boldsymbol{f}_o = \boldsymbol{EV}\{\boldsymbol{H}^{\#} \boldsymbol{\tau}_s + \boldsymbol{N}\boldsymbol{\Phi}\} \tag{13}$$

where $\boldsymbol{E} = [\boldsymbol{I}_3, \ldots, \boldsymbol{I}_3] \in R^{3\times 3n}$. Our former work[14] ensures that we focus on the contact force coinciding with a span vector, when discussing the boundary of total force set. Based on this property, we can introduce the following two constraints.

$$\boldsymbol{S}\boldsymbol{\lambda} \geq \mathbf{o} \tag{14}$$

$$\boldsymbol{S}^* \boldsymbol{\lambda} = \mathbf{o} \tag{15}$$

These constraints mean that each contact force adhere to one of span vectors. From eqs.(12) and (15)

$$\boldsymbol{\Phi} = -\boldsymbol{D}^{-1} \boldsymbol{S}^* \boldsymbol{H}^{\#} \boldsymbol{\tau}_s \tag{16}$$

where $\boldsymbol{D} = \boldsymbol{S}^* \boldsymbol{N}$.

Substituting $\boldsymbol{\Phi}$ into eq.(13) yields

$$\boldsymbol{f}_o = \boldsymbol{EV}(\boldsymbol{I} - \boldsymbol{N}\boldsymbol{D}^{-1}\boldsymbol{S}^*)\boldsymbol{H}^{\#}\boldsymbol{\tau}_s \tag{17}$$

A sufficient condition for lifting up the object is to find $\boldsymbol{\tau}_s$ satisfying the following inequality for all possible combinations of contact forces.

$$c_z^t \boldsymbol{f}_o - m_B g > 0 \tag{18}$$

Once $\boldsymbol{\tau}_s$ is found, we can easily decompose it into $\boldsymbol{K}_\theta$ and $\Delta\boldsymbol{\theta}_p$. For example, if $\boldsymbol{K}_\theta$ is given, then $\Delta\boldsymbol{\theta}_s = \boldsymbol{K}_\theta^{-1}\boldsymbol{\tau}_s$. By using the geometrical relationship between $\Delta\boldsymbol{\theta}_s$ and $\Delta\boldsymbol{\theta}_p$ we can easily compute $\Delta\boldsymbol{\theta}_p$ as well.

3.3 Simulation Results

Fig.5 shows simulation results for a three–fingered robot hand, where each finger has three joints. Each finger consists of the compliant controlled, locked and position–controlled joint, where the lengths of each link are 40[mm], 25[mm] and 25[mm], respectively, and the radius of fingertip is 5[mm]. The object is the cylinder whose mass is $m_B = 0.04[kg]$ and radius is 10[mm]. The friction angle between the surface of object and link is changed as a parameter. Fig.5(b) shows the k_θ–$\Delta\theta_p$ map where $k_{\theta 1} = k_\theta$,

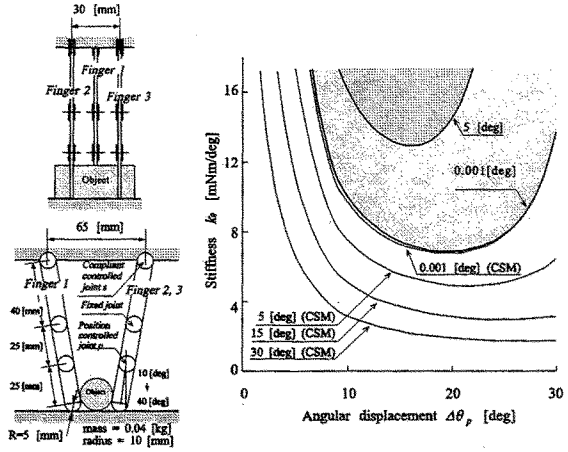

(a) Simulation model (b) Relationship between k_s and $\Delta\theta_p$

Fig. 5: Simulation result

$k_{\theta 2} = k_{\theta 3} = k_\theta/2$ and $\Delta\theta_{p1} = \Delta\theta_{p2} = \Delta\theta_{p3} = \Delta\theta_p$. When we choose the combination of $\Delta\theta_p$ and k_θ within the hatched region whose boundary is given by thick line, it is guaranteed the robot hand can lift up the object from the table, as far as the contact force appears within the friction cone. The region provides us with a sufficient condition, while it may be a bit strict condition. On the other hand, we can determine each contact force uniquely by assuming an appropriate stiffness at each contact point. This approach is often taken in conventional works[15]–[18]. The thin lines given by CSM (Contact Stiffness Model) are obtained under the contact stiffness $\boldsymbol{K}_{Pi} = diag[100000, 100000, 100000]$ ($[N/m]$) for two different friction angles of $\alpha = 5[deg]$ and $1[deg]$. It should be noted that the result under the contact stiffness always provides us with a mild condition, namely the thin line is always lower than that of the sufficient condition obtained along the procedure explain in 3.2. It should be also noted that both thick and thin lines eventually converge to be a single one as $\alpha \to 0$, which guarantees the validity of the simulation. During such a lifting phase, either rolling or sliding motion or a combined motion may occur. We do not care what kind of motion actually happens but have interest only whether the object is lifted up or not.

4 Experimental Results

We implement the *SPCM* into the grasping procedure and execute the grasping experiment for an object placed on a table. The robot hand used in the experiment consists of three finger units and each finger has three links. The length of each link is $40[mm]$, $25[mm]$, and $30[mm]$ in order from the base, respectively, and the radius of each fingertip is about $5[mm]$. Each finger link is driven by wire and a torque sensor is included in each joint. Rotary encoder is also implemented for measuring joint angle. More precise

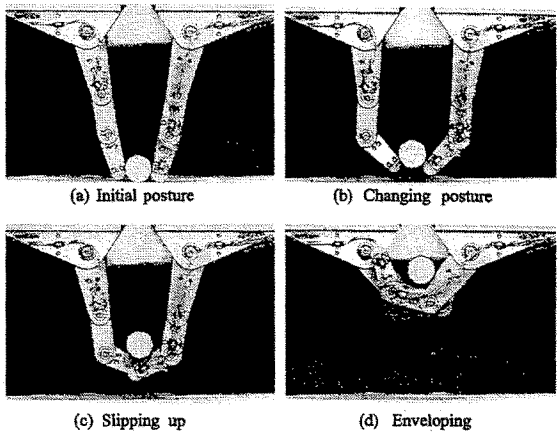

Fig. 6: Experimental results by robot hand

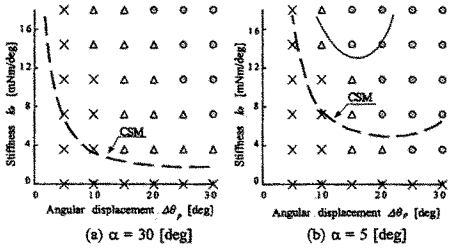

Fig. 7: Experimental results (k_s–$\Delta\theta_p$ map)

information on the robot hand will be obtained in our previous work[19][20].

Fig.6 shows a series of finger postures during a *DAM* by the robot hand, where the first, the second and the third joints are assigned as compliant, locked, and position–controlled joint, respectively. As each position–controlled joint rotates from $15[deg]$ to $80[deg]$, the robot hand lifts up the object from the table (*Rolling–up phase*) as shown in Fig.6(b). Finally, the contact condition between the finger link and the object results in sliding contact (*Wedge–effect phase*) as shown in Fig.6(c). After every fingertip link rotates $80[deg]$, the constant torque control is applied for achieving an enveloping grasp as shown in Fig.6(d).

We also examined the condition for lifting up the object by changing the combination between k_s and $\Delta\theta_p$. Fig.7 shows experimental results, where $\times$, $\triangle$, and $\bigcirc$ denote failure in *DAM*, failure in *DAM* but success in lifting the object, and completely success in *DAM*, respectively. For comparison purpose, Fig.7 also includes simulation results where the real line and the dotted line are the lower boundaries given by the sufficient condition and by the contact stiffness model, respectively. Under a large contact friction $\alpha = 30[deg]$, the sufficient condition discussed in 3.2 does not provide any solution, while we can still find a large area where the robot hand is able to lift up the object. Under a small contact friction $\alpha = 5[deg]$, we can find a small area providing the

sufficient condition, while the solution based on the contact stiffness model supplies a large area where $\boldsymbol{K}_{Pi} = diag[100000, 100000, 100000]$ ($[N/m]$) is given. Overall, we can see the nice coincidence between simulation and experiments in qualitatively. Furthermore, it should be noted that the results based on the contact stiffness model are closely matching with experimental results when the contact stiffness is chosen properly.

5 Conclusion

We discussed the basic working mechanism of the *DAM* and examined the condition leading to the *DAM* by using *SPCM* which is easily implemented for robot hand. As for the condition for lifting up the object, we explored a sufficient condition and compared it with contact stiffness model. We showed that both approaches converge to a single line under frictionless contact. Experimental results were also shown to compare with simulation results. As for further work, we are intending to extend the objects into more general column objects.

This work has been supported by CREST of JST (Japan Science and Technology).

References

[1] M. Cutkosky: "On Grasp Choice, Grasp Models, and the Design of Hands for Manufacturing Tasks," *IEEE Trans. on Robotics and Automation*, Vol. 5, No. 3, JUNE, pp. 269–279, 1989.

[2] G.A. Bekey, H. Liu, R. Tomovic and W. Karplus: "Knowledge-Based Control of Grasping in Robot Hands Using heuristics from human motor skills," *IEEE Trans. on Robotics and Automation*, Vol. 9, No. 6, DECEMBER, pp. 709–722, 1993.

[3] S.B. Kang and K. Ikeuchi: "Toward Automatic Robot Instruction from Perception—Recognizing a Grasp from Observation," *IEEE Trans. on Robotics and Automation*, Vol. 9, No. 4, AUGUST, pp. 432–443, 1993.

[4] T. Iberall, J. Jackson, L. Labbe and R. Zampano: "Knowledge-Based Prehension: Capturing Human Dexterity," *Proc. of the IEEE Int. Conf. on Robotics and Automation*, pp. 82–87, 1988.

[5] F. Saito and K. Nagata: "Interpretation of Grasp and Manipulation from Functional Surfaces," *Proc. of Robotics Symposia*, pp. 113–120, 1999. (In Japanese)

[6] M. Kaneko, Y. Tanaka and T. Tsuji: "Scale-dependent Grasp," *Proc. of the IEEE Int. Conf. on Robotics and Automation*, pp. 2131–2136, 1996.

[7] T. Shirai, M. Kaneko, K. Harada and T. Tsuji: "Scale-Dependent Grasps," *Proc. of the Int. Conf. on Advanced Mechatronics*, pp. 197–202, 1998.

[8] J. Kerr and B. Roth: "Analysis of Multifingered Hands," *International Journal of Robotics Research*, Vol.4, No.4, pp. 3–17, 1986.

[9] S. Hirai and H. Asada: "Kinematics and Statics of Manipulation Using the Theory of Polyhedral Convex Cones," *International Journal of Robotics Research*, Vol.12, No.5, pp. 434–447, 1993.

[10] T. Omata and K. Nagata: "Rigid Body Analysis of the Indeterminate Grasp Force in Power Grasps," *Proc. of the IEEE Int. Conf. on Robotics and Automation*, pp. 1787–1794, 1996.

[11] M. Kaneko and T. Tsuji: "Realization of Enveloping Grasp," *1997 IEEE Int. Conf. on Robotics and Automation (Video Proceeding)*, 1997.

[12] M. Kaneko and K. Tanie : "Contact Point Detection for Grasping an Unknown Object Using Self-Posture Changeability," *IEEE Trans. on Robotics and Automation*, Vol.10, No.3, pp.355–367, 1994.

[13] M. Kaneko and K. Honkawa: "Contact Point and Force Sensing for Inner Link Based Grasps," *Proc. of the IEEE Int. Conf. on Robotics and Automation*, pp. 2809–2814, 1994.

[14] M. Kaneko, K. Harada and T. Tsuji: "A Sufficient Condition for Manipulation of Envelope Family," *Proc. of the IEEE Int. Conf. on Robotics and Automation*, pp. 1060–1067, 2000.

[15] A. Bicchi: "Analysis and Control of Power Grasping, " *Proc. of IEEE/RSJ Int. Workshop on Intelligent Robots and Systems IROS'91*, pp. 691–697, 1991.

[16] A. Bicchi: "Force Distribution in Multiple Whole-Limb Manipulation," *Proc. of the IEEE Int. Conf. on Robotics and Automation*, pp. 196–201, 1993.

[17] W. Stamps and V. Kumar: "On the Stability of Grasped Objects," *IEEE Trans. on Robotics and Automation*, Vol. 12, No. 6, DECEMBER, pp. 904–917, 1996.

[18] P. R. Kuraus, V. Kumar and P. Dupont: "Analysis of Frictional Contact Models for Dynamic Simulation," *Proc. of the IEEE Int. Conf. on Robotics and Automation*, pp. 9769–981, 1998.

[19] N. Imamura, M. Kaneko and T. Tsuji: "Development of Three-Fingered Robot Hand with a New Design Concept," *Proc. of the 6th IASTED Int. Conf. on Robotics and Manufacturing*, pp. 44–49, 1998.

[20] M. Kaneko, K. Yokoi and K. Tanie: "On a New Torque Sensor for Tendon Drive Fingers," *IEEE Trans. on Robotics and Automation*, Vol. 6, No. 4, pp. 501–507, 1990.